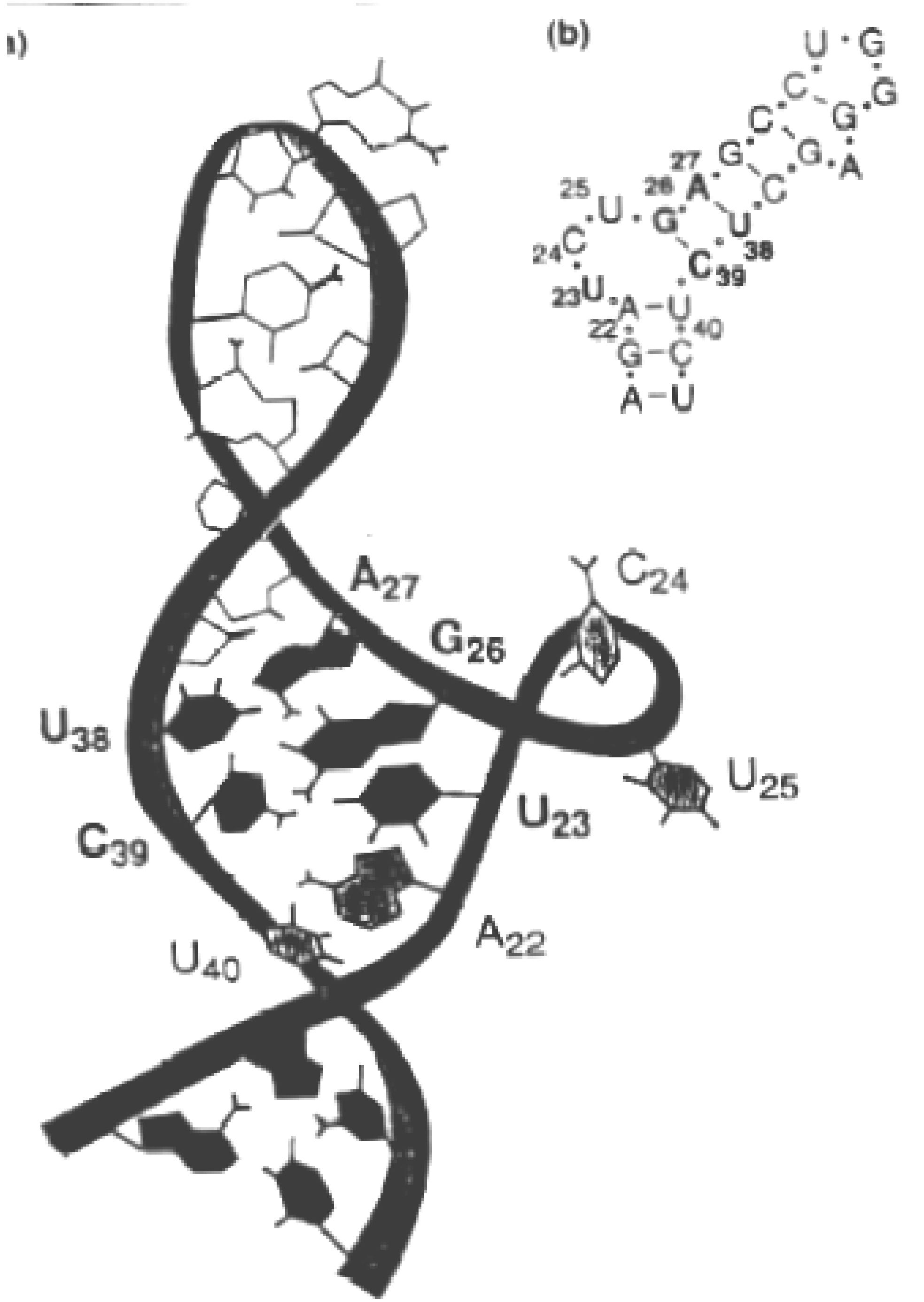

(b)
A27
G26
C24
U25
U38
U23
C39
A22
U40
U · G
C
G
C
G
G
A
25
26
27
24
23
22
38
39
40

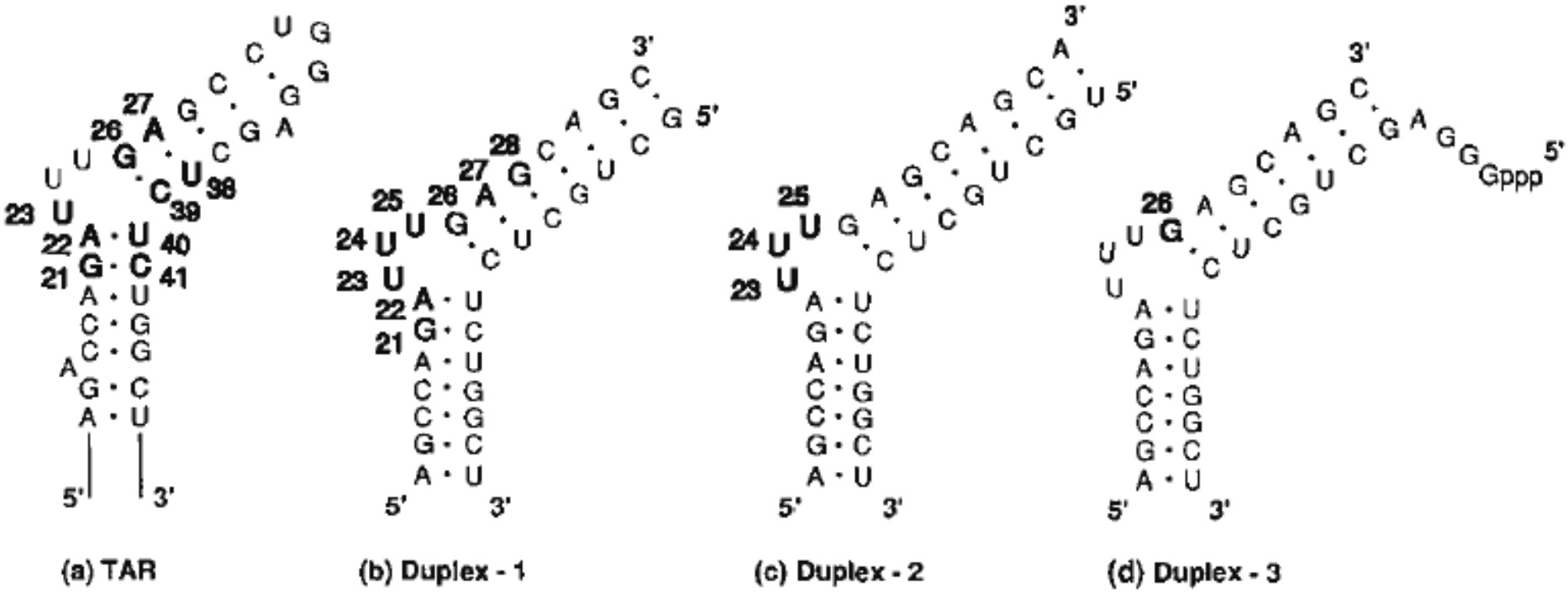

Figure 1. Structure of TAR RNA and synthetic RNA duplexes. (a) Secondary structure of the apex of the TAR stem-loop of HIV-1 (residues 15 to 46). The positions of mutations that cause a reduction in the ability of *tat* to bind TAR RNA (Churcher *et al.*, 1993) are indicated by the residues shown in bold. (b) RNA duplexes containing the U-rich bulge of TAR formed from chemically synthesized 14-mer and 17-mer oligoribonucleotides (duplex-1). Residues 21 to 28 are shown in bold to indicate the positions where base or sugar modifications have been introduced (see the text). (c) RNA duplex containing the U-rich bulge of TAR formed from chemically synthesized 15-mer and 18-mer oligoribonucleotides (duplex-2). (d) RNA duplex containing the U-rich bulge of TAR formed from chemically synthesized 17-mer and transcribed 18-mer oligoribonucleotides (duplex-3).

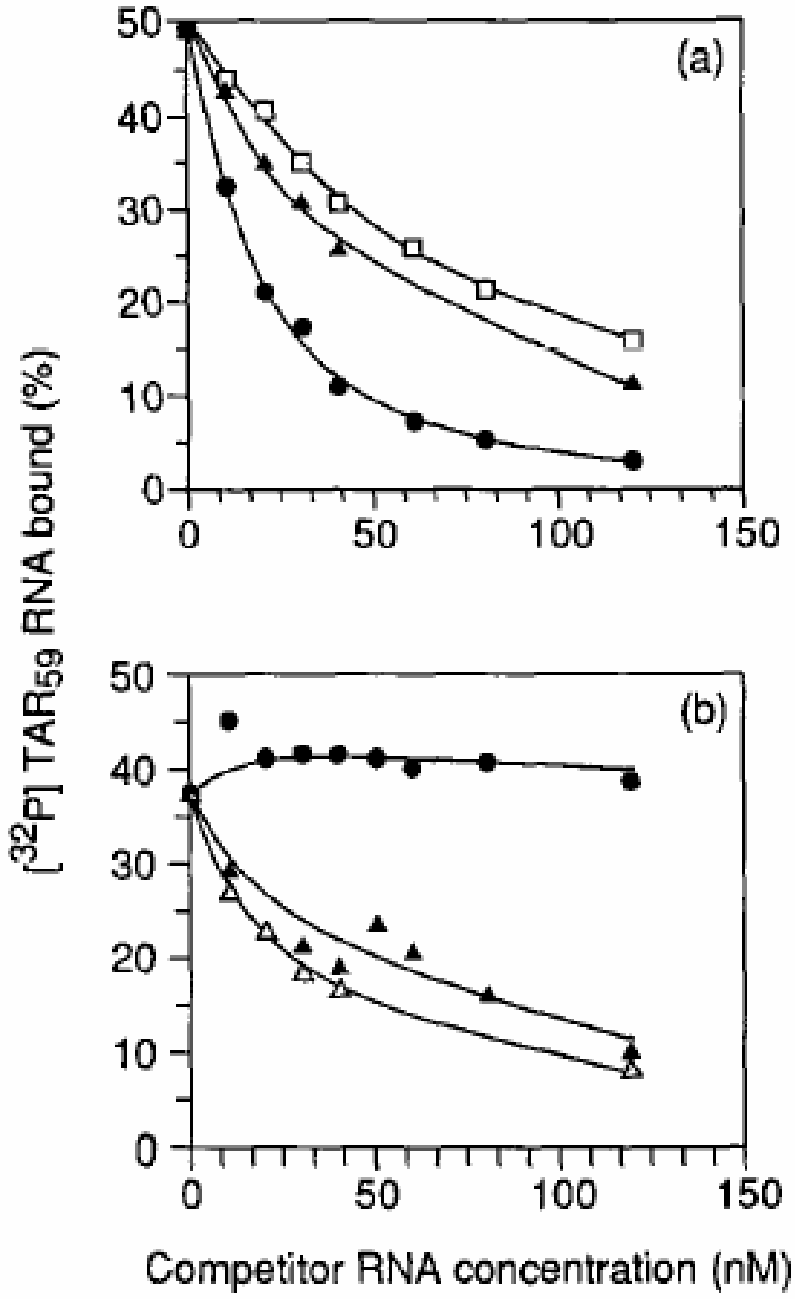

Figure 2. Competition nitrocellulose filter binding curves using ^{32}P-labelled TAR_{59} RNA transcript competed against the following RNA molecules: (a) (●), Unlabelled TAR_{59} RNA; (▲), duplex-1 RNA; (□) duplex-2 RNA. (b) (▲), Duplex-1 RNA; (△), duplex-1 RNA carrying dT_{23}; (●), duplex-1 RNA carrying $\Delta U_{23\ 25}$.

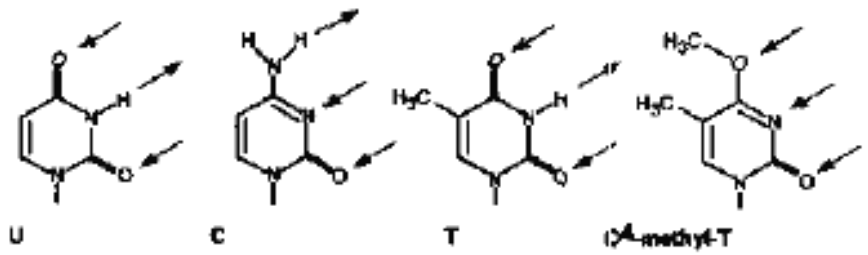

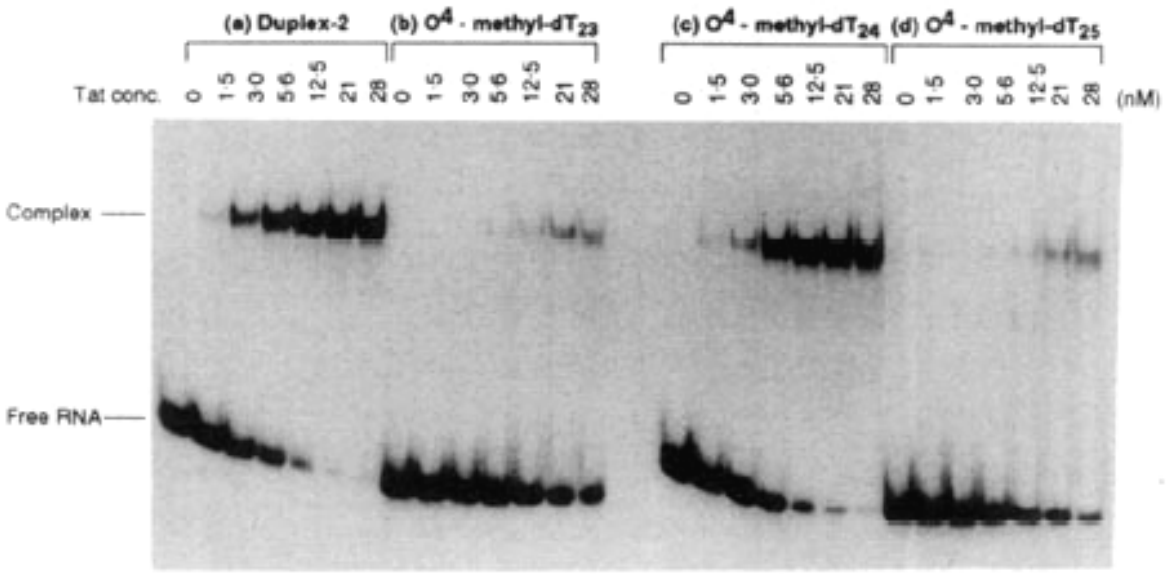

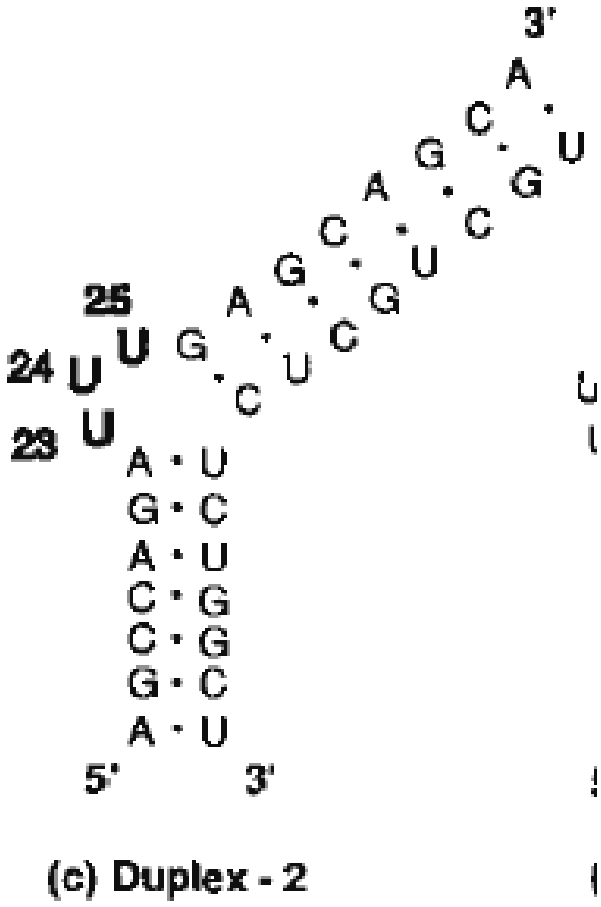

Figure 3. Effect of O^4-methyl-dT substitution of *uridines in the U-rich bulge on tat* binding to duplex-2

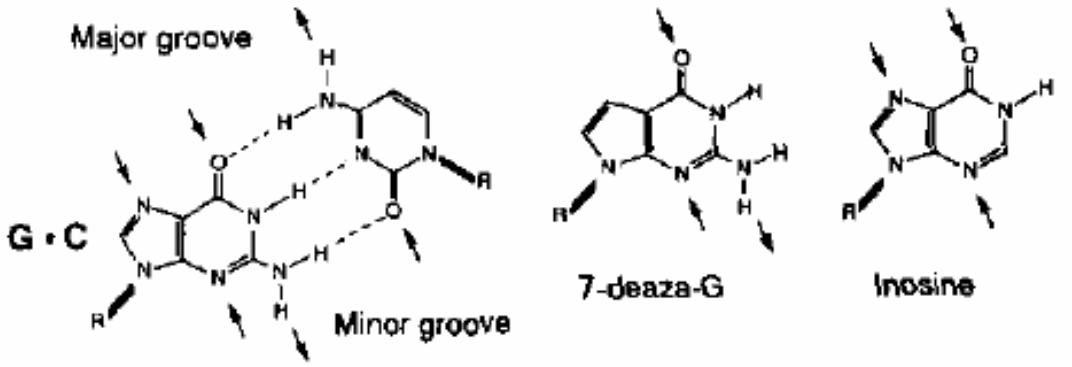
Major groove
G • C
Minor groove
7-deaza-G
Inosine

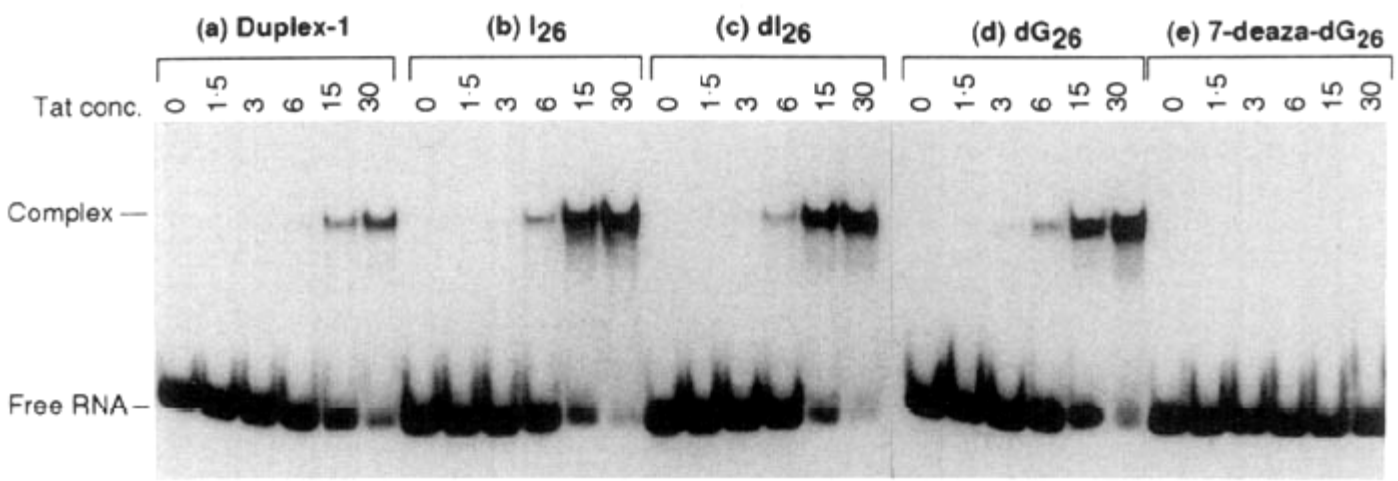
(a) Duplex-1
(b) I26
(c) dI26
(d) dG26
(e) 7-deaza-dG26
Tat conc.
0 1·5 3 6 15 30
Complex
Free RNA

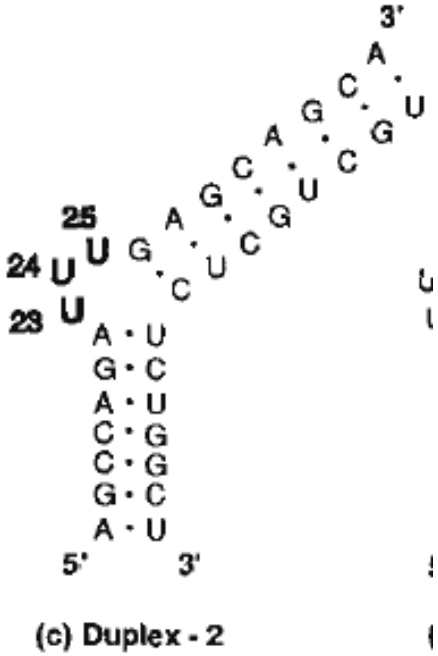
3'
25
24 U
23 U
A • U
G • C
A • U
C • G
C • G
G • C
A • U
5'
3'
(c) Duplex - 2

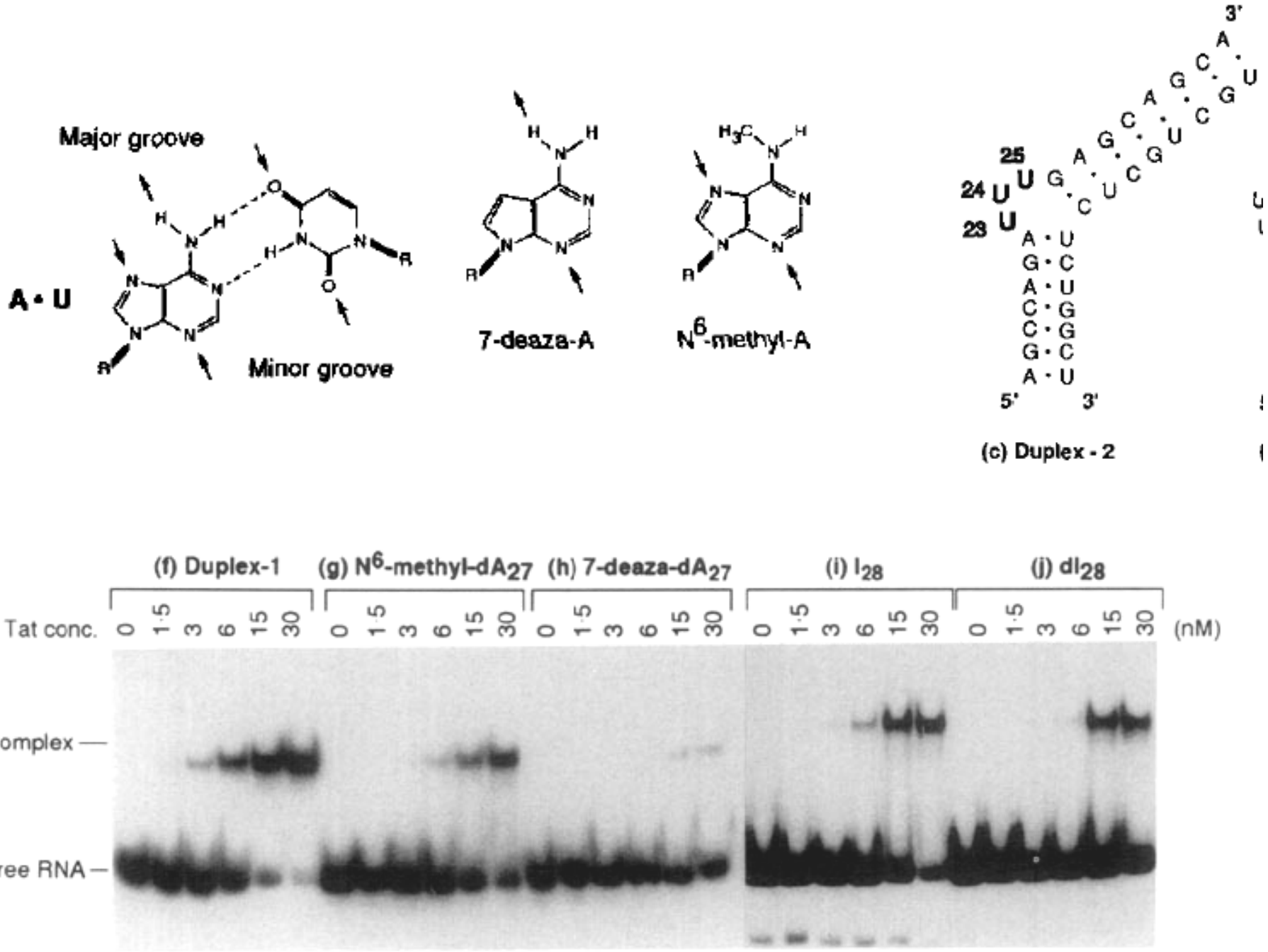
Major groove
A • U
Minor groove
7-deaza-A
N6-methyl-A
3'
25
24 U
23 U
5'
3'
(c) Duplex - 2
(f) Duplex-1
(g) N6-methyl-dA27
(h) 7-deaza-dA27
(i) I28
(j) dI28
Tat conc.
0 1·5 3 6 15 30
(nM)
Complex
Free RNA

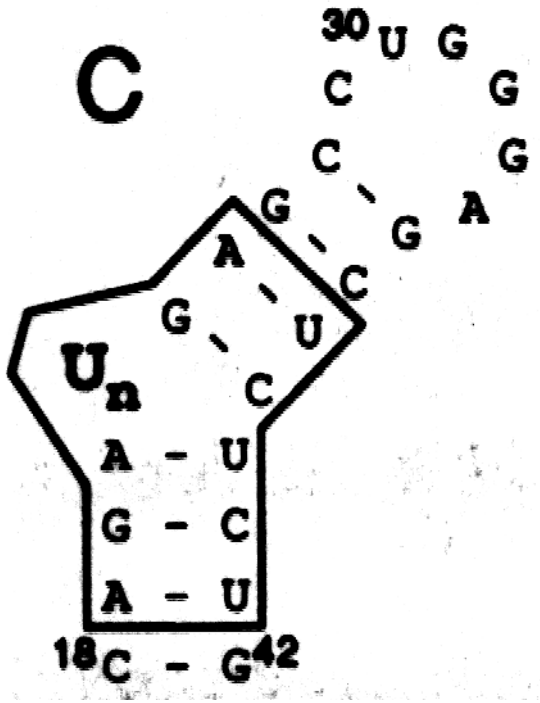

n	K_{rel}
0†	≥40
1†	8 ± 2
2	0.6 ± .1
3†	0.9 ± .1
4	1.6 ± .2
3 *reverse*	~15